Journal of
MATERIALS RESEARCH

Welcome Comments Help

Etching of polycrystalline diamond films by electron beam assisted plasma

Koji Kobashi, Shigeaki Miyauchi, Koichi Miyata, and Kozo Nishimura
Kobe Steel, Ltd., Electronics Research Laboratory, 5-5, Takatsuka-dai 1-chome, Nishi-ku, Kobe 651-22, Japan

Jorge J. Rocca
Department of Electrical Engineering, Colorado State University, Fort Collins, Colorado 80523

(Received 20 November 1995; accepted 4 June 1996)

Polycrystalline diamond films were processed in a direct current plasma produced by a self-focused electron beam using combinations of H_2, O_2, and He as the processing gas. The film surfaces were observed by scanning electron microscopy, and characterized by x-ray photoelectron spectroscopy. It was found that for the case in which O_2 was included in the processing gas, a high density of etch pits appeared on (100) faces of diamond grains, and oxygen was either physisorbed or chemisorbed at the film surface. It was demonstrated that the etching apparatus used was capable of forming at least a 5-μm wide pattern of polycrystalline diamond film.

I. INTRODUCTION

Etching of diamond films has been investigated by many researchers using various techniques which are summarized[1–11] in Table I. However, direct-current (dc) plasma has not been used for etching of diamond, and only few attempts have been done to fabricate patterns of diamond films by etching.[12] The present paper describes a novel technique for etching polycrystalline diamond films using dc plasma. The apparatus used was based on an invention of a self-focused electron beam generator for gas lasers by Rocca *et al.*,[21–23] and will be called an Electron Beam-Assisted Plasma Etching (EBAPE) system. It is featured by a cathode with a concave surface and a high operational pressure up to about 10 Torr (1 Torr = 133 Pa). In the present study, a combination of O_2, H_2, and He was used as the processing gas. The film surfaces before and after plasma treatment were observed by scanning electron microscopy (SEM), and characterized by x-ray photoelectron spectroscopy (XPS). Finally, a pattern formation of diamond film by etching was demonstrated using the same apparatus.

II. EXPERIMENTAL

The structure of the EBAPE system is schematically shown in Fig. 1. The inner diameter of the chamber is 200 mm. The cathode head was aluminum with a concave surface, whose diameter and curvature were 75 mm and 200 mm, respectively. The cathode head was mounted on a water-cooled copper stage which was linked to a dc generator. The chamber wall as well as the specimen holder were grounded. The aluminum surface of the cathode was oxidized during the operation either by the processing gas or the residual air and water vapor in the chamber. Owing to the concave cathode surface, the plasma sheath was curved along the cathode surface, which resulted in a self-focused electron beam without an opposing anode. The diamond specimen was placed on a water-cooled stage which was spaced about 150 mm from the cathode. The chamber had been evacuated by a rotary pump down to about 0.01 Torr before processing. For the processing gas, combinations of O_2, H_2, and He were used with the total gas flow rate of about 100 cc/min.

Figure 2 shows a photograph of the EBAPE system under operation using 0.97 cc/min O_2 and 26 cc/min He at a gas pressure of 0.25 Torr, a dc voltage of 2.9 kV, and a current of 200 mA. The cathode is seen on the right-hand side of the circular window, while the specimen is placed on the holder on the left-hand side. From the cathode toward the specimen, there exists a red cathode glow region, a dark space, and a bright blue negative glow discharge region. Electrons are accelerated in the plasma sheath region between the cathode and the negative glow discharge region. After several experiments, it was found that only a 55-mm diameter area of the cathode surface was oxidized. Ignoring the current due to ions, it was

TABLE I. Etching methods of diamond films.

Etching technique	Processing gases	References
Thermal	O_2, air	1, 2, 3, 4
Hot filament	O_2, H_2O, O_2 + Ar	5, 6, 7
RF plasma	CF_4, O_2, O_2 + Ar	8, 9, 10, 11, 12
Microwave plasma	1 air	13, 14
ECR plasma	O_2, BCl_3, SF_6, O_2 + Ar	15, 16, 17
Excimer laser	Cl_2, NO_2, NH_3	18, 19, 20

 © 1996 Materials Research Society

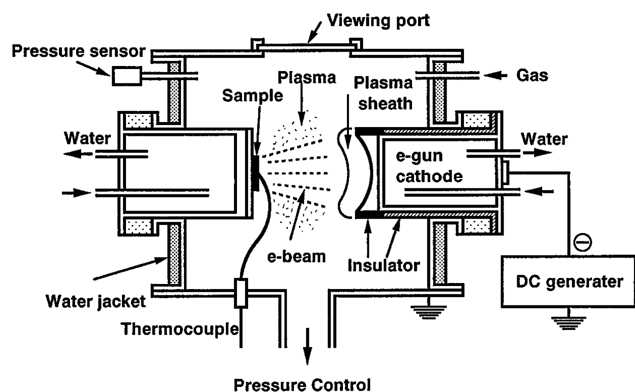

FIG. 1. Schematic structure of the EBAPE system.

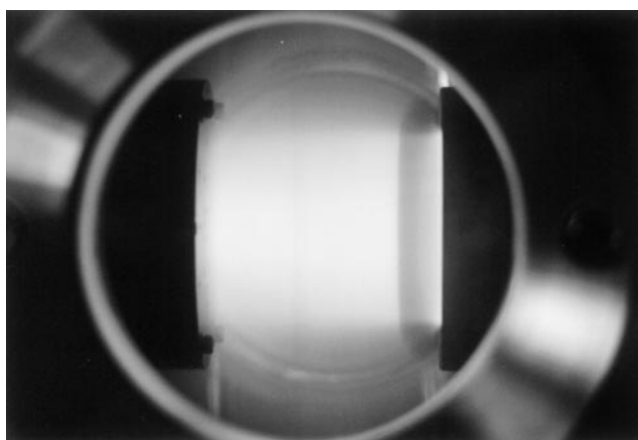

FIG. 2. The EBAPE apparatus under operation.

estimated that a flux of about 1.3×10^{16} electrons was generated per unit surface area of the cathode per second.

If the elastic scattering cross section of electron with a He atom, 10^{-15} to 10^{-16} cm^2 is used, the mean free path of electrons is estimated to be less than 3 mm in He gas at 1 Torr. Therefore, it is unlikely that the electrons emitted from the cathode directly hit the specimen without collision with the processing gas molecules at this pressure. However, as seen in Fig. 2, it appears as if the plasma flows out from the cathode to the specimen continuously, although the plasma is less uniform for 1.2 kV at 1 Torr. Therefore, it seems that successive ionization steps are occurring in the plasma, and if this is the case, the specimen is actually hit by the electrons existing in the vicinity of the specimen surface. Note, however, that when the He gas pressure is 0.02 Torr, the mean free path of electrons is about 150 mm, which is comparable to the distance between the cathode and the specimen. Therefore, the specimen can be directly hit by electrons generated by the cathode.

In the present experiments, high an low power modes were used, as shown in Tables II and III. In the high power mode using the processing parameters given in Table II, the temperature of the specimen, monitored by an optical pyrometer under an assumption that the emissivity is unity, increased quickly to about 700 °C within about two minutes after the ignition of plasma. On the other hand, in the low power mode, the substrate did not reach a temperature higher than 600 °C, the lower sensing limit of the optical pyrometer used. Thus, in order to determine the substrate temperature, a separate experiment was undertaken using a thermocouple in contact with the substrate. It was found that after three minutes from the plasma ignition, the substrate temperature went up to about 200 °C, and then became constant.

For most cases, plasma treatments were done for five minutes, as seen in Tables II and III. However, when an O_2–He mixed gas was used as the processing gas (Samples C and H), the experiments were terminated only after three minutes, as the etching rate of diamond was too high.

Regarding diamond film preparation, about 1.5-μm thick films were grown on low-resistivity Si substrates using a NIRIM-type microwave plasma chemical vapor deposition (MPCVD) reactor described in Ref. 24. The growth conditions were also described in the reference. A SEM photograph of the film surface is shown in Fig. 3. It is seen that the film surface consisted of diamond grains with both triangular (111) and square (100) faces. On the other hand, a 5-μm thick diamond film was used for pattern formation. In this case, the film was grown by a different reactor described in Ref. 25. The source gas was a mixture of 5% CH_4 and 95% H_2. An XPS spectrum in the valence band region of an *as grown* diamond film synthesized by MPCVD is

TABLE II. Experimental conditions for the high power mode.

Sample	Reaction gases (%)			Power	Pressure	Duration	Morphology	XPS
	O_2	H_2	He	(kV/mA)	(Torr)	(min)		
A	0.0	44.5	55.5	1.2/500	1.0	15	Fig. 5(a)	Fig. 4(b)
B	4.3	40.0	55.7	1.3/480	1.0	15	Fig. 5(b)	Fig. 4(c)
C	0.7	0.0	99.3	1.5/480	1.0	3	Fig. 5(c)	Fig. 4(d)
D	0.0	0.0	100	1.25/400	1.0	15	Fig. 5(d)	Fig. 4(e)
E	0.0	0.0	100	5.5/60	0.02	15	Fig. 5(e)	Fig. 4(f)

TABLE III. Experimental conditions for the low power mode.

Sample	Reaction gases (%) O_2	H_2	He	Power (kV/mA)	Pressure (Torr)	Duration (min)
F	0.0	44.5	55.5	0.7/200	1.0	15
G	4.3	40.0	55.7	0.8/180	1.0	15
H	0.7	0.0	99.3	0.85/170	1.0	3
I	0.0	0.0	100	0.70/200	1.0	15
J	0.0	0.0	100	2.7/5.5	0.02	15

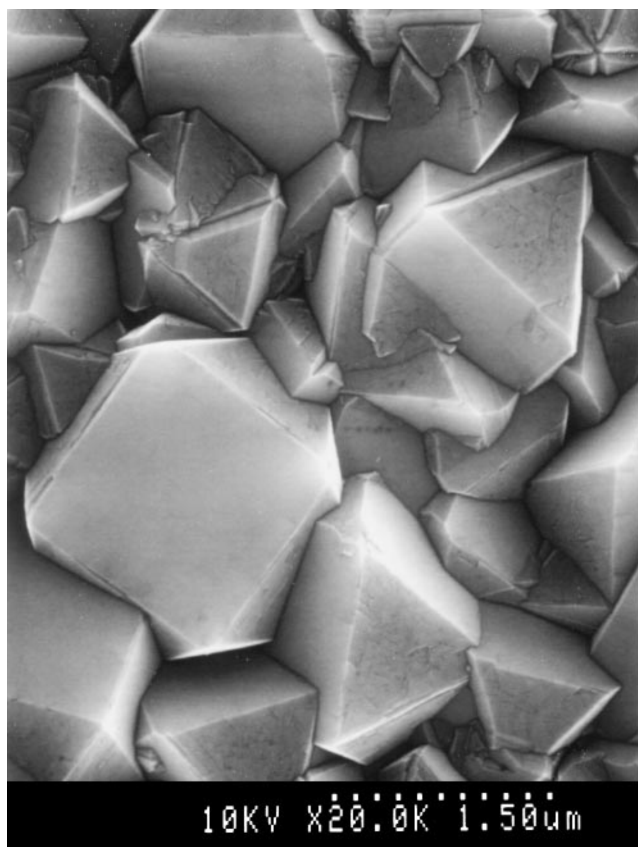

FIG. 3. SEM photograph of *as grown* film synthesized by a NIRIM-type MPCVD reactor.

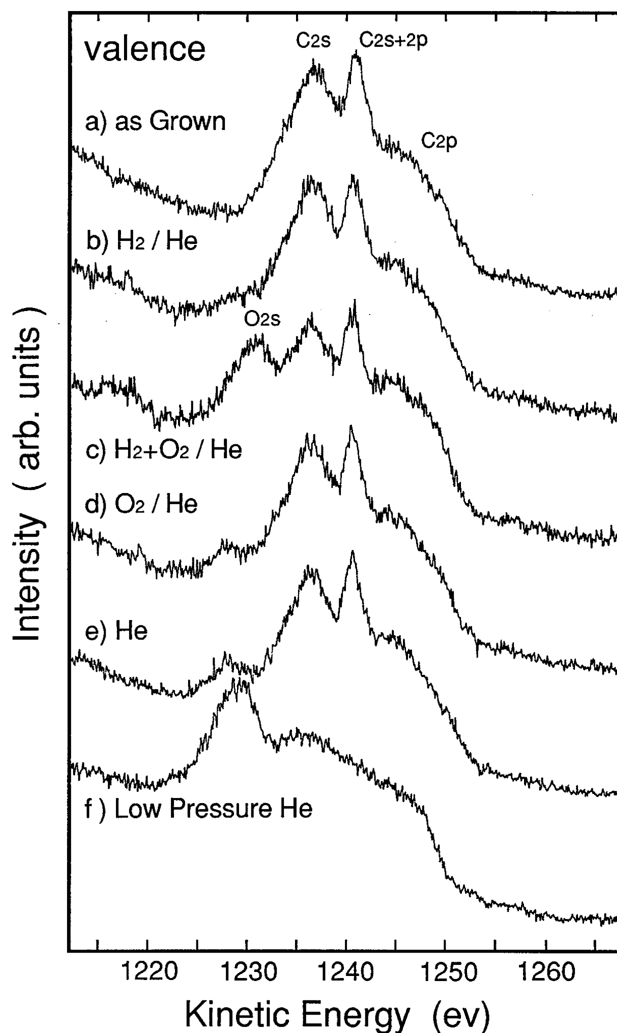

FIG. 4. Valence band XPS spectra of the plasma-processed specimen: (a) Sample A, (b) Sample B, (c) Sample C, (d) Sample D, (e) Sample E, and (f) Sample F. For processing conditions, see Table II.

shown in Fig. 4(a). Since Fig. 4(a) is a typical spectrum of diamond, it was concluded that the synthesized film was a high quality diamond.

III. RESULTS AND DISCUSSION

A. High power mode

Figures 5(a)–5(c) show SEM photographs of the diamond films after the plasma treatments using H_2, O_2–H_2, and O_2, all diluted with He. These samples are labeled as Samples A–C in Table II, respectively. Control experiments, labeled as Samples D and E in Table II, were done using He at 1 and 0.01 Torr, and the SEM results are shown in Figs. 5(d) and 5(e), respectively.

As seen in Fig. 5(a), the surface structure was little modified by the hydrogen plasma treatment (Sample A) except that small but dense etch pits appeared on both (100) and (111) faces of the diamond grains. However, diamond surfaces were strongly eroded by adding O_2 to the processing gas [Sample B, Fig. 5(b)]: high density etch pits appeared on (100) faces, while (111) faces were uniformly etched. The etch pits on (100) faces were more prominent when O_2–He was used as the processing gas [Sample C, Fig. 5(c)]. Etch pits also appeared by a He plasma treatment at 1 Torr [Sample D, Fig. 5(d)]. This is presumably due to etching by a residual oxygen and water vapor left in the chamber, because the back pressure of the EBAPE system was

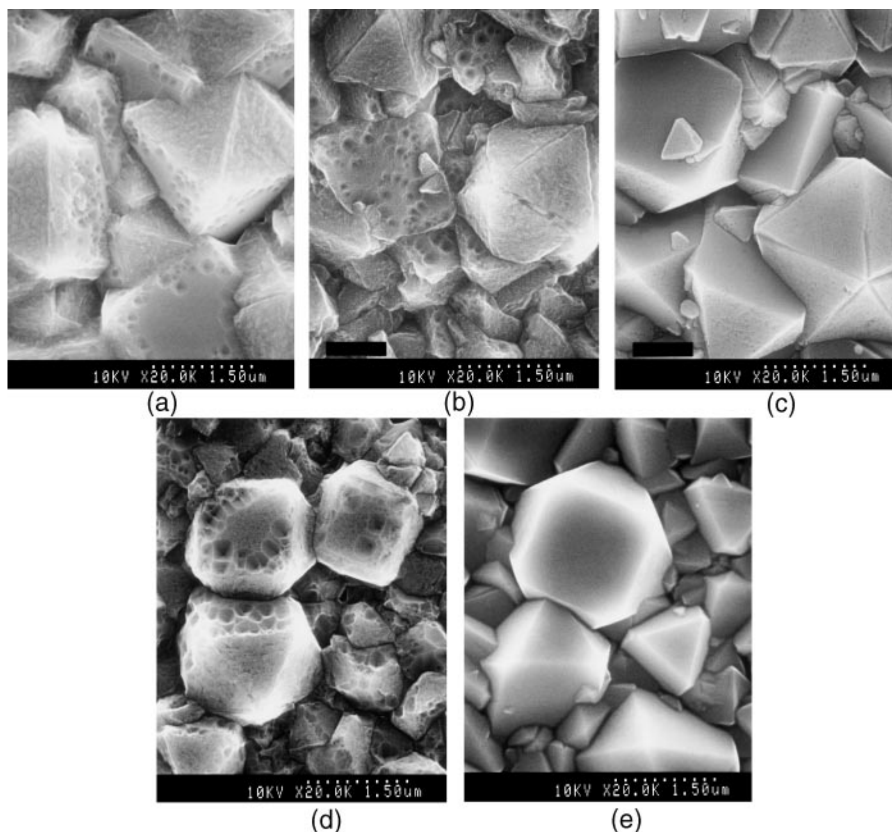

FIG. 5. SEM photographs of the plasma-treated diamond films: (a) Sample B, (b) Sample C, (c) Sample D, (d) Sample E, and (e) Sample F.

only 0.01 Torr. However, when the He pressure was 0.02 Torr [Sample E, Fig. 5(e)], there was no remarkable change in the film morphology, and no etch pits were observed.

XPS spectra in the valence region of the plasma-treated samples are shown in Figs. 4(b)–4(f). The spectrum of H_2 plasma-treated Sample A [Fig. 4(b)] has the same structure as that of *as grown* film, consisting of the bands at 1235, 1240, and 1245 eV due to C_{2s}, C_{2s+2p}, and C_{2p}, respectively. This indicated that the surfaces of both *as grown* and H_2-plasma treated films consist of only sp^3 bonds. An extra band appeared at 1230 eV when the diamond film was treated by a H_2–O_2–He plasma, which was assigned to O_{2s}. This band was smaller for Samples C and D, even though the diamond film surfaces were more strongly eroded by the plasma. The XPS spectrum of Sample E, treated by He plasma at low pressure (0.02 Torr), was typical for graphite, indicating that the diamond surface was graphitized by electron bombardment, because the mean free path of electrons at this pressure is comparable to the cathode-specimen distance. The other indications of the surface graphitization was seen in the binding energy spectrum of XPS (data not shown), where a weak shoulder appeared at 290 eV, which was assigned to a $\pi - \pi^*$ transition in sp^2 bonded networks.

B. Low power mode

In the lower power mode, both the electric current and the dc bias voltage were reduced, and thus the temperature, determined by a separate experiment using a thermocouple, was not higher than 200 °C. There was no remarkable change in the surface morphology of the plasma-treated Samples F to J, compared with the corresponding Samples B to E in the high power mode. Similarly, XPS valence spectra of Samples F to J showed no marked difference from those of Figs. 4(b)–4(f) obtained from Samples B to E.

C. Pattern formation

In order to see if the present etching technique can be used for a pattern formation of diamond films, a gold film mask with a 7-μm wide pattern was deposited on a 5-μm thick diamond film using a standard photolithography method. Then, the specimen was processed using 4.3 cc/min O_2, 40 cc/min H_2, and 55 cc/min He, at 1.0 Torr and 800 °C for 60 min.

A cross section of the pattern after etching is shown in Fig. 6. It was found that the diamond film was only 5-μm wide, indicating that it was severely undercut by the plasma. In other SEM views (not shown), a columnar structure was observed on the etched vertical

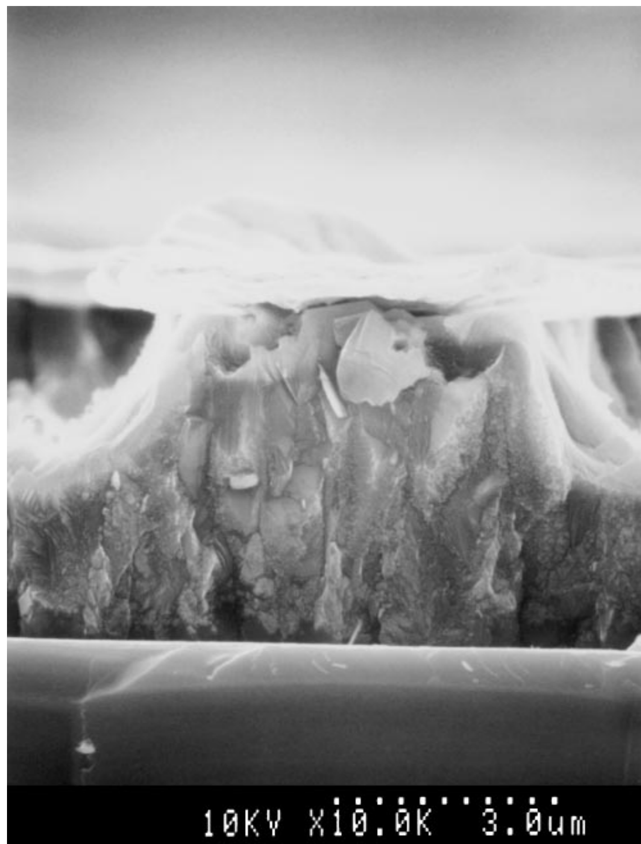

FIG. 6. Cross-sectional view of patterned diamond film. The plate on top is the gold film mask.

side of the film. This means that grain boundaries were preferentially etched more than diamond grains under the processing conditions employed. From Fig. 6, the etching rate was estimated to be 40 nm/min. These results indicated that the etching was isotropic even though the electron beam has the directionality.

IV. CONCLUSION

Diamond films were treated by a dc plasma of combinations of O_2, H_2, and He using the EBAPE system. It was found that etch pits appeared on (100) faces except for the case of the He plasma treatment at 0.02 Torr. There was no appreciable difference between the low power and high power modes. A 5-μm diamond film pattern was achieved by the present etching method, although the etching was significantly isotropic. It is expected that the present method will be useful not only for pattern formation but also for cleaning surfaces of CVD diamond films.

REFERENCES

1. C. E. Johnson, M. A. S. Hasting, and W. A. Weimer, J. Mater. Res. **5**, 2320 (1990).
2. R. R. Nimmagadda, A. Joshi, and W. L. Hsu, J. Mater. Res. **5**, 2445 (1990).
3. K. Tankala, T. DebRoy, and M. Alan, J. Mater. Res. **5**, 2483 (1990).
4. L. Plano, S. Yokota, and K. V. Ravi, Proc. Electrochem. Soc. **89-12**, 380 (1989).
5. N. Uchida, T. Kurita, H. Ohkishi, K. Uematsu, and K. Saito, J. Cryst. Growth **114**, 565 (1991).
6. N. Uchida, T. Kurita, K. Uematsu, and K. Saito, J. Mater. Sci. Lett. **9**, 249 (1990).
7. N. Uchida, T. Kurita, K. Uematsu, and K. Saito, J. Mater. Sci. Lett. **9**, 251 (1990).
8. G. S. Sandhu and W. K. Chu, Appl. Phys. Lett. **55**, 437 (1989).
9. A. Joshi and R. Nimmagadda, J. Mater. Res. **6**, 1484 (1991).
10. K. Kobayashi, N. Mutsukura, and Y. Machi, Thin Solid Films **200**, 139 (1991).
11. O. Dorsch, K. Holzner, M. Werner, E. Obermeier, R. E. Harper, C. Johnson, P. R. Chalker, and I. M. Buckley-Golder, Diamond and Related Mater. **2**, 1096 (1993).
12. M. I. Landstrass, M. A. Plano, M. A. Moreno, S. McWilliams, L. S. Pan, D. R. Kania, and S. Han, Diamond and Related Mater. **2**, 1033 (1993).
13. Y. Sato and M. Kamo, Surf. Coat. Technol. **39–40**, 183 (1989).
14. R. Ramesham and B. H. Loo, J. Electrochem. Soc. **139**, 1988 (1992); Errata, J. Electrochem. Soc. **139**, 2874 (1992).
15. S. A. Grot, R. A. Ditizio, G. Sh. Gildenblat, A. R. Badzian, and S. J. Fonash, Appl. Phys. Lett. **61**, 2326 (1992).
16. S. A. Grot, G. Sh. Gildenblat, and A. R. Badzian, IEEE Electron Device Lett. **13**, 462 (1992).
17. S. J. Pearton, A. Katz, F. Rein, and J. R. Lothian, Electron. Lett. **28**, 822 (1992).
18. N. N. Efremow, M. W. Geis, D. C. Flanders, G. A. Lincoln, and N. P. Economou, J. Vac. Sci. Technol. B **3**, 416 (1985).
19. M. Rothschild, C. Arnone, and D. J. Ehrlich, J. Vac. Sci. Technol. B **4**, 310 (1986).
20. C. Johnson, P. R. Chalker, I. M. Buckley-Golder, P. J. Marsden, and S. W. Williams, Diamond and Related Mater. **2**, 829 (1993).
21. C. A. Moore, J. J. Rocca, T. Johonson, G. J. Collins, and P. E. Russell, Appl. Phys. Lett. **43**, 290 (1983).
22. T. R. Thompson, J. J. Rocco, K. Emery, P. K. Boyer, G. J. Collins, Appl. Phys. Lett. **43**, 777 (1983).
23. J. J. Rocco, J. W. Meyer, M. R. Farrell, and G. J. Collins, J. Appl. Phys. **56**, 790 (1984).
24. K. Kobashi, K. Nishimura, Y. Kawate, and T. Horiuchi, Phys. Rev. B **38**, 4067 (1988).
25. U.S. patent 4 940 015.